Uncertainty-aware Accumulated Local Effects (UALE) for quantifying the heterogeneity of instance-level feature effects

Anonymous Author
Anonymous Institution

Abstract

Accumulated Local Effects (ALE) is a popular explainable AI method that quantifies how a feature influences the decisions of a model, handling well feature correlations. In case of complex interactions between features, instance-level feature effects may deviate from the ALE curve. It is crucial to quantify this deviation, namely, the uncertainty of the global effect. In this work, we define Uncertainty-aware ALE (UALE) to quantify and visualize, on a single plot, both the average effect and its uncertainty. We show that UALE quantifies uncertainty effectively, even in case of correlated features. We also note that as in ALE, UALE's approximation requires partitioning the feature domain into non-overlapping intervals (bin-splitting). The average effect and the uncertainty are computed from the instances that lie in each bin. We formally prove that to achieve an unbiased approximation of the uncertainty in each bin, bin-splitting must follow specific constraints. Based on this, we propose a method to determine the optimal intervals, balancing the estimation bias and variance. We demonstrate, through synthetic and real datasets, (a) the advantages of modeling the uncertainty with UALE compared to alternative methods and (b) the effectiveness of UALE's appropriate bin splitting for accurately approximating of the average effect and its uncertainty.

1 INTRODUCTION

Recently, Machine Learning (ML) has been widely adopted in mission critical domains, such as healthcare and finance. In such high-stakes areas, it is important not only to provide accurate predictions but also meaningful explanations. For this reason, there is an increased interest in Explainable AI (XAI). XAI literature distinguishes between local and global methods (Molnar et al., 2020a). Local methods provide instance-level explanations, i.e., explain the prediction for a specific instance, whereas global methods summarize the entire model behavior, aggregating the instance-level explanations into a single interpretable outcome, usually a number or a plot.

A popular class of global XAI are feature effect (FE) methods (Grömping, 2020) that quantify the average (across all instances) effect of a single feature on the output. There are three widely-used FE methods: *Partial Dependence Plots* (PDP) (Friedman, 2001), *Marginal Plots* (MP) (Apley and Zhu, 2020) and *Accumulated Local Effects* (ALE) (Apley and Zhu, 2020). ALE is established as the state-of-the-art, since PDP and MP have been criticized (Baniecki et al., 2021; Grömping, 2020) of providing misleading explanations in case of correlated input features.

In case of complex interactions between features, the instance-level (local) feature effects may exhibit significant deviation, aka heterogeneity, from the aggregated (global) explanation, a phenomenon known as aggregation bias (Mehrabi et al., 2021). We call this deviation *the uncertainty of the global effect*[1]. Aggregation bias leads to ambiguities. For example, a feature with zero average effect may indicate (a) no effect on the output or (b) highly positive effect for some instances and highly negative for some others. As a result, there is a need for FE methods to quantify the deviation of instance-level explanations, in addition to the average effect. In the case of PDP, such deviation is visualized via the Individual Conditional Explanations (ICE) (Goldstein et al., 2015). ICE plots, however, have the same limitations as PDP in case of correlated features. No method to quantify the deviation of instance-level effects has been proposed for ALE.

In this work, we propose UALE, a global feature-effect method that extends ALE for modeling the uncertainty of

Preliminary work. Under review by AISTATS 2023. Do not distribute.

[1] In the paper, the *uncertainty of the global effect* and the *heterogeneity of instance-level effects* are used interchangeably and refer to the deviation of instance-level (local) effects from the averaged feature effect curve (global).

the feature effect. Our method handles well cases with correlated features. As in ALE, we provide an interval-based formulation of UALE. This formulation partitions the feature domain into non-overlapping intervals (bin-splitting) and defines the average effect (bin-effect) and its uncertainty (bin-uncertainty). We use this formulation to provide an UALE approximation. As we formally prove, a fixed equi-width partitioning that does not consider the characteristics of the instance-level effects, which is the case in ALE approximation, may lead to an erroneous (biased) estimation of the uncertainty. Therefore, we propose a variable-width partitioning that leads to an unbiased approximation. The contributions of this paper are:

- A global feature effect method (UALE) that quantifies both the average effect and its uncertainty, i.e., the heterogeneity of instance-level effects.
- An unbiased approximation of the uncertainty through an appropriate variable-size bin partitioning of the feature domain.
- The evaluation of UALE on both synthetic and real datasets.

The implementation of our method and the code for reproducing all the experiments is provided along with the manuscript and will become publicly available upon acceptance.

2 BACKGROUND AND RELATED WORK

In the rest of the paper, we use following notation. Let $\mathcal{X} \in \mathbb{R}^d$ be the d-dimensional feature space, $\mathcal{Y} \in \mathbb{R}$ the target space and $f(\cdot) : \mathcal{X} \to \mathcal{Y}$ the black-box function. We use index $s \in \{1, \dots, d\}$ for the feature of interest and $c = \{1, \dots, d\} - s$ for the set with all other indexes. For convenience, we denote the feature vector $\mathbf{x} = (x_1, \cdots, x_s, \cdots, x_D)$ with $(x_s, \mathbf{x}_c)$ and the corresponding random variables $X = (X_1, \cdots, X_s, \cdots, X_D)$ with (X_s, X_c). The training set is $\mathcal{D} = \{(\mathbf{x}^i, y^i)\}_{i=1}^N$ sampled i.i.d. from the distribution $\mathbb{P}_{X,Y}$. Finally, we use $f^{<\texttt{method}>}(x_s)$ for denoting the effect of the s-th, where $<$ `method` $>$ indicates the particular method in use, e.g., ALE.

2.1 Feature Effect Methods

The three well-known feature effect methods are: *Partial Dependence Plots* (PDP), *Marginal Plots* (MP) and *Accumulated Local Effects* (ALE). PDP formulates the global FE as an expectation over the distribution of X_c, i.e., $f^{\texttt{PDP}}(x_s) = \mathbb{E}_{X_c}[f(x_s, X_c)]$, whereas MP as an expectation over the distribution of $X_c|X_s$, i.e., $f^{\texttt{MP}}(x_s) = \mathbb{E}_{X_c|x_s}[f(x_s, X_c)]$. Both methods suffer from misestimations when features are correlated. PDP integrates over unrealistic instances and MP computes aggregated effects, i.e., imputes the combined effect of sets of features to a single feature (Apley and Zhu, 2020).

ALE overcomes these problems. Specifically, ALE defines the local effect of the s-th feature at a specific point $(z, \mathbf{x}_c)$ of the input space $\mathcal{X}$ with the partial derivative $f^s(z, \mathbf{x}_c) = \frac{\partial f}{\partial x_s}(z, \mathbf{x}_c)$. All the local explanations at z are then weighted by the conditional distribution $p(\mathbf{x}_c|z)$ and are averaged, to produce the averaged effect $\mu(z)$. ALE plot is the accumulation of the averaged local effects:

$$f^{\texttt{ALE}}(x_s) = \int_{x_{s,min}}^{x_s} \underbrace{\mathbb{E}_{X_c|X_s=z}\left[f^s(z, X_c)\right]}_{\mu(z)} \partial z \qquad (1)$$

where $x_{s,min}$ is the minimum value of the s-th feature.

2.2 Heterogeneity Of Instance-Level Effects

The global effect is computed as an expectation over local (instance-level) effects. In addition to this global effect, it is important to know to what extent the local effects deviate from the global explanation.

ICE plots and similar methods (e.g., d-ICE plots (Goldstein et al., 2015)) provide a set of curves illustrated on top-of PDP. Each curve corresponds to one instance of the dataset, $f_i^{\texttt{ICE}}(x_s) = f(x_s, \mathbf{x}_c^i)$. The user then visually observes if the curves are homogeneous, i.e., all instances have similar effect plots, and to what extent they deviate from the PDP. Some approaches (Herbinger et al., 2022; Britton, 2019; Molnar et al., 2020b) automate the aforementioned visual exploration, by grouping ICE plots into clusters. Unfortunately, these methods are subject to the failure modes of PDPs in cases of correlated features.

Other approaches, like H-Statistic (Friedman and Popescu, 2008), Greenwell's interaction index (Greenwell et al., 2018) or SHAP interaction values (Lundberg et al., 2018) quantify interactions between the input features. A strong interaction is an implicit indication of the existence of heterogeneous effects. These methods, however, do not quantify directly the level of heterogeneity.

To the best of our knowledge no work exist so far that quantifies the heterogeneous effects (uncertainty) based on the formulation of ALE.

2.3 ALE Approximation

ALE is estimated from the available dataset instances. (Apley and Zhu, 2020) proposed to divide the domain of the s-th feature in K equal-size bins and estimate the bin-effects from the instances that lie in each bin after setting the s-th feature at the bin limits:

$$\hat{f}^{\texttt{ALE}}(x_s) = \sum_{k=1}^{k_x} \frac{1}{|\mathcal{S}_k|} \sum_{i:\mathbf{x}^i \in \mathcal{S}_k} \left[f(z_k, \mathbf{x}_c^i) - f(z_{k-1}, \mathbf{x}_c^i) \right] \tag{2}$$

where k_x the index of the bin such that $z_{k_x-1} \leq x_s < z_{k_x}$ and $\mathcal{S}_k$ is the set of the instances of the k-th bin, i.e. $\mathcal{S}_k = \{\mathbf{x}^i : z_{k-1} \leq x_s^i < z_k\}$. (Gkolemis et al., 2022) proposed the Differential ALE (DALE) that computes the local effects on the training instances using auto-differentiation:

$$\hat{f}^{\texttt{DALE}}(x_s) = \Delta x \sum_{k=1}^{k_x} \frac{1}{|\mathcal{S}_k|} \sum_{i:\mathbf{x}^i \in \mathcal{S}_k} f^s(\mathbf{x}^i) \tag{3}$$

Their method has significant computational advantages and allows the recomputation of the accumulated effect with a modified bin-splitting with near-zero additional computational cost. Moreover, by avoiding the use of artificial samples at the bin limits DALE allows the use of wider bins without out-of-distribution sampling. In both cases, the approximations partition the feature domain in K equally-sized bins, without considering the underlying local effects.

3 Uncertainty-Aware ALE (UALE)

We define UALE and provide an interval-based formulation that partitions the feature domain into non-overlapping intervals (bin-splitting) and defines the bin-effect and the bin-uncertainty. Then, we present UALE approximation, formally proving the bin-splitting requirements for an unbiased estimation of the uncertainty. Based on this, we present an optimization method to determine an appropriate variable-width partitioning. Figure 1 illustrates an UALE visualization. The upper plot shows the ALE curve and its uncertainty as the shaded area around the curve. The lower plot shows the bins obtained after UALE's partitioning and the effects and the uncertainty per bin.

3.1 UALE Definition and Interval-Based Formulation

We quantify the uncertainty of the local effects at $x_s = z$ with the standard deviation of the local explanations, $\sigma(z)$, where:

$$\sigma^2(z) = \mathbb{E}_{X_c|X_s=z} \left[\left(f^s(z, X_c) - \mu(z) \right)^2 \right] \tag{4}$$

The uncertainty emerges from (a) the feature correlations and (b) the implicit feature interactions of the black-box function. We also define the accumulated uncertainty at x_s, as the accumulation of the standard deviation of the local effects:

$$f_\sigma^{\texttt{ALE}}(x_s) = \int_{x_{s,min}}^{x_s} \sigma(z) \partial z \tag{5}$$

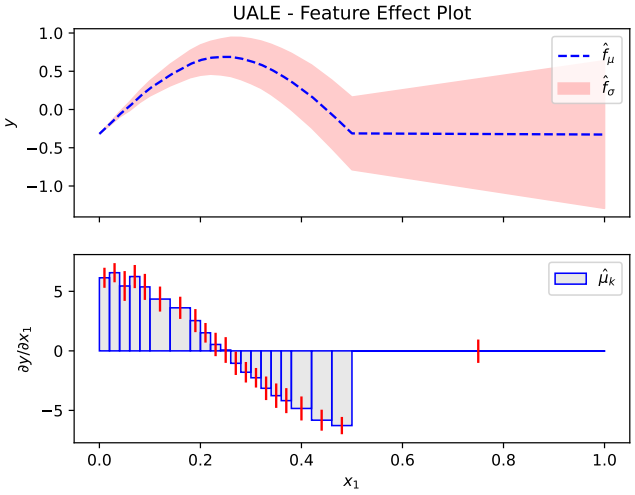

Figure 1: Illustration of UALE feature effect plot.

UALE defines the effect as a pair that consists of the average effect and the uncertainty $(\mu(z), \sigma(z))$. For visualizing it, we use the accumulated average effect, as defined in Eq. (1), and the accumulated uncertainty, as defined in Eq. (5). Figure 1 illustrates a toy example, where $x_1 \sim \mathcal{U}(0,1)$ and $x_2 \sim \mathcal{N}(0, \sigma_2^2)$ and the black-box function is $f(\mathbf{x}) = \sin(2\pi x_1) + x_1 x_2$.

For the interval-based formulation, we define the bin-effect $\mu(z_1, z_2)$ and the bin-uncertainty $\sigma(z_1, z_2)$ as:

$$\mu(z_1, z_2) = \mathbb{E}_{z \sim \mathcal{U}(z_1, z_2)}[\mu(z)] = \frac{\int_{z_1}^{z_2} \mu(z) \partial z}{z_2 - z_1} \tag{6}$$

$$\sigma^2(z_1, z_2) = \mathbb{E}_{z \sim \mathcal{U}(z_1, z_2)}[\sigma^2(z)] = \frac{\int_{z_1}^{z_2} \sigma^2(z) \partial z}{z_2 - z_1} \tag{7}$$

Intuitively, if we randomly draw a point z^* from a uniform distribution $z^* \sim \mathcal{U}(z_1, z_2)$, the bin-effect (Eq. (6)) and the bin-uncertainty (Eq. (7)) are the expected average effect and the expected uncertainty, respectively. Also, if we denote as $\mathcal{Z}$ the sequence of $K+1$ points that partition the domain of the s-th feature into K variable-size intervals, i.e. $\mathcal{Z} = \{z_0, \ldots, z_K\}$, we provide the interval-based formulation of UALE:

$$\tilde{f}_{\mathcal{Z},\mu}^{\texttt{ALE}}(x_s) = \sum_{k=1}^{k_x} \mu(z_{k-1}, z_k)(z_k - z_{k-1}) \tag{8}$$

$$\tilde{f}_{\mathcal{Z},\sigma}^{\texttt{ALE}}(x_s) = \sum_{k=1}^{k_x} \sigma(z_{k-1}, z_k)(z_k - z_{k-1}) \tag{9}$$

where k_x is the index of the bin such that $z_{k_x-1} \leq x_s < z_{k_x}$. Eq. (8) and Eq. (9) are piecewise-linear approximation of Eq. (1) and Eq. (5).

3.2 UALE Interval-Based Approximation

For approximating the bin-effect and the bin-uncertainty, we use the set $\mathcal{S}_k$ of dataset instances with the s-th feature lying inside the k-th bin, i.e., $\mathcal{S}_k = \{\mathbf{x}^i : z_{k-1} \leq x_s^i < z_k\}$. The bin-effect is approximated with,

$$\hat{\mu}(z_{k-1}, z_k) = \frac{1}{|\mathcal{S}_k|} \sum_{i:\mathbf{x}^i \in \mathcal{S}_k} \left[f^s(\mathbf{x}^i) \right] \tag{10}$$

which is an unbiased estimator of Eq. (6) under the assumption that the points are uniformly distributed inside the interval. The approximation for the uncertainty (Eq. (7)) from the available instances is defined as follows:

$$\hat{\sigma}^2(z_{k-1}, z_k) = \frac{1}{|\mathcal{S}_k|} \sum_{i:\mathbf{x}^i \in \mathcal{S}_k} \left(f^s(\mathbf{x}^i) - \hat{\mu}(z_1, z_2) \right)^2 \tag{11}$$

In the Appendix **??**, we show that $\hat{\sigma}^2(z_1, z_2)$ is an unbiased estimator of $\sigma_*^2(z_1, z_2) = \frac{\int_{z_1}^{z_2} \mathbb{E}_{X_c|X_s=z}\left[(f^s(z, X_c) - \mu(z_1, z_2))^2\right] \partial z}{z_2 - z_1}$. In Theorem 3.1 we prove that in the general case, $\sigma_*^2(z_1, z_2) \geq \sigma^2(z_1, z_2)$, so $\hat{\sigma}^2(z_1, z_2)$ is an overestimation of the bin uncertainty.

Theorem 3.1. *If we define (a) the residual $\rho(z)$ as the difference between the expected effect at z and the bin-effect, i.e $\rho(z) = \mu(z) - \mu(z_1, z_2)$ and (b) $\mathcal{E}(z_1, z_2)$ as the mean squared residual of the bin, i.e. $\mathcal{E}(z_1, z_2) = \frac{\int_{z_1}^{z_2} \rho^2(z) \partial z}{z_2 - z_1}$, then it holds*

$$\sigma_*^2(z_1, z_2) = \sigma^2(z_1, z_2) + \mathcal{E}^2(z_1, z_2) \tag{12}$$

Proof. The proof is at Appendix **??**. □

We refer to $\mathcal{E}^2(z_1, z_2)$ as bin-error. Based on Theorem3.1, the estimation is unbiased only when $\mathcal{E}^2(z_1, z_2) = 0$.

3.3 Bin-Splitting

The quality of UALE approximation is affected by (a) the population of samples in each bin and (b) the error term $\mathcal{E}(z_1, z_2)$ of each bin. On the one hand, we favor a partitioning of the feature domain in large-bins to allow a robust estimation of $\hat{\mu}(z_1, z_2), \hat{\sigma}(z_1, z_2)$ from a sufficient population of samples. On the other hand, we want to minimize the cumulative bin-error, i.e., $\mathcal{E}_{\mathcal{Z}}^2 = \sum_{k=1}^{K} \mathcal{E}^2(z_1, z_2) \Delta z_k$, where $\mathcal{Z} = \{z_0, \cdots, z_K\}$ and $\Delta z_k = z_k - z_{k-1}$. We search for a partitioning that balances this trade-off.

Corollary 3.1.1 shows that minimizing $\mathcal{E}_{\mathcal{Z}}^2$ is equivalent to minimizing $\sum_{k=1}^{K} \sigma_*^2(z_{k-1}, z_k) \Delta z_k$, which can be directly estimated from $\sum_{k=1}^{K} \hat{\sigma}^2(z_{k-1}, z_k) \Delta z_k$.

Corollary 3.1.1. *A bin-splitting $\mathcal{Z}$ that minimizes the accumulated error if and only if it also minimizes $\sum_{k=1}^{K} \sigma_*^2(z_1, z_2) \Delta z_k$*

Proof. The proof is based on the observation that $\sum_{k=1}^{K} \sigma^2(z_{k-1}, z_k) \Delta z_k = \sigma^2(z_0, z_K)(z_K - z_0)$ which is independent of the bin-splitting. A more detailed proof is provided in the Appendix **??**. □

Based on the above, we set-up the following optimization problem:

$$\begin{aligned} \min_{\mathcal{Z}=\{z_0,\ldots,z_K\}} \quad & \mathcal{L} = \sum_{k=1}^{K} \tau_k \hat{\sigma}^2(z_{k-1}, z_k) \Delta z_k \\ \text{where} \quad & \Delta z_k = z_k - z_{k-1} \\ & \tau_k = 1 - \alpha \frac{|S_k|}{N} \\ \text{s.t.} \quad & |\mathcal{S}_k| \geq N_{\texttt{PPB}} \\ & z_0 = x_{s,min} \\ & z_K = x_{s,max} \end{aligned} \tag{13}$$

The objective $\mathcal{L}$ searches for a partitioning $\mathcal{Z}^* = \{z_0^*, \ldots, z_K^*\}$ with low aggregated error $\mathcal{E}_{\mathcal{Z}}^2$. In case of many partitionings with similar aggregate-error, the term τ_K favors the partitioning with more points per bin, i.e., with wider bins. The constraint of at least $N_{\texttt{PPB}}$ points per bin sets the lowest-limit for a *robust* estimation. The user can choose to what extent they favor the creation of wide bins through (a) the parameter α that controls the discount τ_k and (b) the parameter $N_{\texttt{PPB}}$ that sets the minimum population per bin. For providing a rough idea, in our experiments we set $\alpha = 0.2$ which means that the discount ranges between $[0\%, 20\%]$ and $N_{\texttt{PPB}} = \frac{N}{20}$, where N is the dataset size.

For solving the optimization problem of Eq.13 we add some constraints. First, we set a threshold K_{max} on the maximum number of bins which, in turn, defines the minimum bin-width, i.e. $\Delta x_{min} = \frac{x_{s,max} - x_{s,min}}{K_{max}}$. Based on that, we restrict the bin-limits to the multiples of the minimum width, i.e. $z_k = k \cdot \Delta x_{min}$, where $k \in \{0, \cdots, K_{max}\}$. In this discretized solution space, we find the global optimum using Dynamic Programming.

To define the solution, we use two indexes. The index $i \in \{0, \ldots, K_{max}\}$ denotes the points of the partitioning (z_i) and the index $j \in \{0, \ldots, K_{max}\}$ denotes the j-th multiple of the minimum step, i.e., $x_j = x_{s,min} + j \cdot \Delta x_{min}$. The recursive cost function $T(i, j)$ computes the cost of setting z_i to x_j:

$$\mathcal{T}(i, j) = \min_{l \in \{0,\ldots,K_{max}\}} \left[\mathcal{T}(i-1, l) + \mathcal{B}(x_l, x_j) \right] \tag{14}$$

The term $\mathcal{B}(x_l, x_j)$ denotes the cost of creating a bin with limits $[x_l, x_j)$:

$$\mathcal{B}(x_l, x_j) = \begin{cases} \infty, & \text{if } x_j > x_l \text{ or } |\mathcal{S}_{(x_j,x_l)}| < N \\ 0, & \text{if } x_j = x_l \\ \hat{\sigma}^2(x_j, x_l), & \text{if } x_j \leq x_l \end{cases} \tag{15}$$

The optimal solution is given by solving $\mathcal{L} = \mathcal{T}(K_{max}, K_{max})$ and keeping track of the sequence of steps.

4 SIMULATION EXAMPLES

We perform a two-fold evaluation of UALE. First, (Section 4.1) compares UALE with PDP-ICE, the main feature effect method that also quantifies the heterogeneity of instance-level effects. Second, (Section 4.2) evaluates UALE approximation, i.e., compares UALE's optimal bin-splitting against the fixed-size alternative.

4.1 UALE vs PDP-ICE

This a qualitative example to highlight that PDP-ICE is vulnerable to misleading estimations of both the average effect and the uncertainty, even in case of a simple black-box function, as opposed to UALE.

Example set-up. We use the data generating distribution $p(\mathbf{x}) = p(x_3)p(x_2|x_1)p(x_1)$, where $x_1 \sim \mathcal{U}(0,1)$, $x_2 = x_1$ and $x_3 \sim \mathcal{N}(0, \sigma_3^2)$, and the following function,

$$f(\mathbf{x}) = \begin{cases} f_1(\mathbf{x}) + \alpha f_2(\mathbf{x}) & \text{if } f_1(\mathbf{x}) < \frac{1}{2} \\ \frac{1}{2} - f_1(\mathbf{x}) + \alpha f_2(\mathbf{x}) & \text{if } \frac{1}{2} \leq f_1(\mathbf{x}) < 1 \\ \alpha f_2(\mathbf{x}) & \text{otherwise} \end{cases} \tag{16}$$

where $f_1(\mathbf{x}) = a_1 x_1 + a_2 x_2$ and $f_2(\mathbf{x}) = x_1 x_3$. The part f_1 is a linear function of the two correlated features, x_1, x_2, and f_2 is an interaction term between the two non-correlated, x_1, x_3. We evaluate the effect computed by UALE and PDP-ICE in three cases; (a) without interaction ($\alpha = 0$) and equal weights ($a_1 = a_2$), (b) without interaction ($\alpha = 0$) and different weigths ($a_1 \neq a_2$) and (c) with interaction ($\alpha > 0$) and equal weights ($a_1 = a_2$).

In the general case, evaluating feature effect methods is a challenging task, because there is no unique ground-truth feature effect and uncertainty and each method defines the effect in a different way. To deal with this, we exploit two characteristics of the above set-up. First, in $p(\mathbf{x})$ it holds that $x_1 = x_2$. Therefore, knowing x_1 or x_2, we know the closed-form of $f(\mathbf{x})$, too. For example, if $a_1 = a_2 = 1$ and $0 \leq x_1 < \frac{1}{4}$, then $f_1(\mathbf{x}) < \frac{1}{2}$, so $f(\mathbf{x}) = f_1(\mathbf{x}) + \alpha f_2(\mathbf{x})$, i.e., the first branch of Eq. 16. Afterwards, we can determine the ground-truth. In the example above, if $a = 0$, then $f(\mathbf{x}) = x_1 + x_2$ and therefore the ground-truth effect of x_1 is $f^{\mathcal{GT}}(x_1) = x_1$ in the corresponding interval, i.e. $x_1 \in [0, \frac{1}{4})$. For the uncertainty, we use the fact that under no-interactions, $a = 0$, the uncertainty must be zero (no heteregoneity). We discuss separately the case with $a > 0$. Finally, we also demonstrate that UALE's approximation is accurate, due to the bin splitting that we propose.

(a) No Interaction, Equal weights. Here, $\alpha = 0$ (no interaction) and the $a_1 = a_2 = 1$ (equal weights). We examine only the effect of feature x_1, because it is exactly the same as with x_2. Based on the discussion above, the ground truth effect $f_\mu^{\mathtt{GT}}(x_1)$ is: x_1 in $[0, \frac{1}{4}]$, $-x_1$ in $[\frac{1}{4}, \frac{1}{2}]$ and 0 in $[\frac{1}{2}, 1]$. Because x_1 does not interact with any other feature, the uncertainty is $f_{\sigma^2}^{\mathcal{GT}}(x_1) = 0$. In Figure 2, we observe that PDP effect is wrong and ICE plots show heterogeneous effects. In contrast, UALE models correctly both the average effect and the absence of uncertainty. Finally, we observe that UALE's bin-splitting leads (a) to an accurate uncertainty estimation (near-zero cumulative bin-error $\mathcal{E}_\mathcal{Z}$) and (b) an easier interpretation, creating three wide bins, i.e. $[0, \frac{1}{4}), [\frac{1}{4}, \frac{1}{2}), [\frac{1}{2}, 1)$, that correspond to the piecewise-linear regions of the effect.

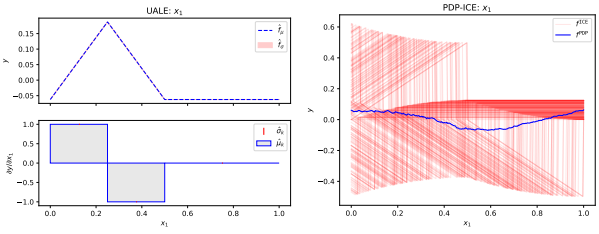

Figure 2: No interaction, Equal weights: Feature effect for x_1 using UALE (Left) and PDP-ICE (Right).

(b) No Interaction, Non-Equal Weights. Here, $\alpha = 0$ (no interaction), $a_1 = 2$ and $a_2 = \frac{1}{2}$ (non-equal weights). The non-equal weights have implications at both the gradient and the interval of the piece-wise linear regions, i.e., $f_\mu^{\mathtt{GT}}(x_1)$ is: $2x_1$ in $[0, \frac{1}{5}]$, $-2x_1$ in $[\frac{1}{5}, \frac{2}{5}]$ and 0 in $[\frac{2}{5}, 1]$. As before, the ground-truth uncertainty is $f_{\sigma^2}^{\mathcal{GT}}(x_1) = 0$ because x_1 does not interact with any other feature. In Figure 3, we observe that PDP estimation is opposite to the ground-truth effect, i.e. negative in the region $[0, \frac{1}{5})$, positive in $[\frac{1}{5}, \frac{2}{5})$, and the ICE erroneously implies the existence of heterogeneous effects. As before, UALE quantifies correctly the ground truth effect, the zero-uncertainty and partitions the x_1 domain into wide bins that facilitate the interpretation and create a zero cummulative bin-error $\mathcal{E}_\mathcal{Z}$ approximation.

(c) With Interaction, Equal weights. Here, we activate the interaction term, i.e., $a = 1$, keeping the weights equal $a_1 = a_2 = 1$ and $\sigma_3^2 = \frac{1}{4}$. In this case, it is not straightforward to define the ground-truth effect for fea-

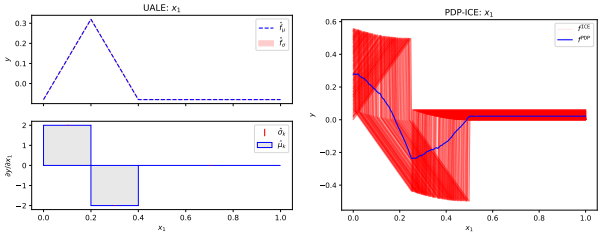

Figure 3: No interaction, Different weights: Feature effect for x_1 using UALE (Left) and PDP-ICE (Right).

tures x_1, x_3, because the interaction term provokes heterogeneous instance-level effects, i.e., the instance-level effect of x_1 depend on the unknown value of x_3 and vice-versa. We observe that UALE's feature effects are quite intuitive. The average effect of x_1 is the same with the Example (a) with an added uncertainty, reflecting the uncertainty about the instance-level effects which is the standard deviation of x_3, i.e., $\sigma_3 = \frac{1}{2}$. The effect of x_3 is only due to the interaction term, therefore, the instance-level effects, $\frac{\partial f}{\partial x_3} = x_1$, follow $p(x_1) \sim \mathcal{U}(0,1)$ which has $\mu_{x_1} = \frac{1}{2}$ and $\sigma_{x_1} = \frac{1}{4}$. This is reflected, in UALE's estimations of Figure 4. We note that PDP-ICE provide (a) for x_1 a near-zero average effect plot, which is not intuitive and (b) for x_3 a plot that, roughly, matches with UALE.

For x_2, as in Example (a), the effect is $f_\mu^{\texttt{GT}}(x_2)$ is: x_2 in $[0, \frac{1}{4}]$, $-x_2$ in $[\frac{1}{4}, \frac{1}{2}]$ and 0 in $[\frac{1}{2}, 1]x_2$ and it has zero-uncertainty, $f_\sigma^{\texttt{GT}}(x_2) = 0$, since x_2 does not appear in any interaction term. We confirm that UALE computes it correctly whereas PDP-ICE fail in both the average effect and the uncertainty.

Discussion. The above experiments show that UALE models correctly and estimates accurately both the average effect and its uncertainty. We also observed that UALE's variable-size bin-splitting method that we propose, leads to (a) an accurate approximation of the uncertainty and (b) favoring wider bins we facilitate the interpretation of both the average effect and the uncertainty. In contrast, PDP-ICE provides misleading explanations in many cases, by ignoring dependence relationships between features. The examples above do not cover the case of an interaction term between correlated features, for example a term $x_1 x_2$, because in this case there is an open debate about the ground-truth effect (Grömping, 2020).

4.2 UALE vs Fixed-Size Approximation

In this simulation, we focus on illustrating the advantages of UALE's variable-size bin-splitting against fixed-size one.

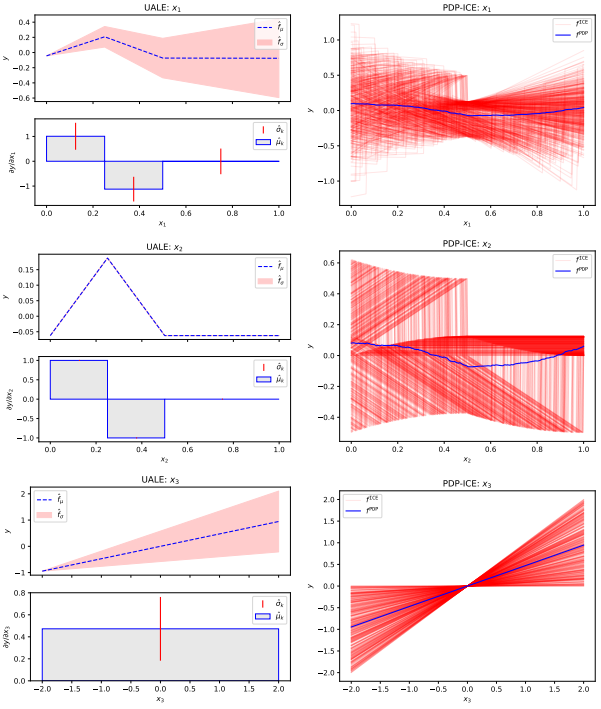

Figure 4: With interaction, equal weights: From top to bottom, feature effect for features $\{x_1, x_2, x_3\}$ using UALE (left column) and PDP-ICE (right column).

Example set-up. The purpose of this experiment is two-fold. First, we show that UALE provides an approximation which is close to the best fixed-size approximation, among all possible K. Second, we illustrate that UALE favors the creation of wider intervals when possible to facilitate the interpretation of the average effect and its uncertainty.

To measure the accuracy of the approximation, we generate a dataset with dense sampling ($N = 10^6$) and we use dense fixed-size bins ($K = 10^3$). We treat this estimation as the ground-truth UALE. Afterwards, we generate fewer samples ($N = 500$) and we compare the fixed-size estimation (for several K) against UALE's.

We sample from $p(\mathbf{x}) = p(x_2|x_1)p(x_1)$ where $x_1 \sim \mathcal{U}(0,1)$ and $x_2 \sim \mathcal{N}(x_1, \sigma_2^2 = 0.5)$. We denote as $\mathcal{Z}^* = \{z_0^*, \cdots, z_K^*\}$ UALE's partitioning, and with $\mathcal{Z}^{\texttt{K}}$ the fixed-size splitting with K bins. The evaluation is based on the Mean Absolute Error (MAE) of the bin effect μ and of the uncertainty σ accross bins, i.e.,

$$\mathcal{L}^{\mu} = \frac{1}{|\mathcal{Z}| - 1} \sum_{k \in \mathcal{Z}} |\mu(z_{k-1}, z_k) - \hat{\mu}(z_{k-1}, z_k)| \quad (17)$$

$$\mathcal{L}^{\sigma} = \frac{1}{|\mathcal{Z}| - 1} \sum_{k \in \mathcal{Z}} |\sigma(z_{k-1}, z_k) - \hat{\sigma}(z_{k-1}, z_k)| \quad (18)$$

We obtain the ground truth bin-effect, $\mu(z_{k-1}, z_k)$ and the ground truth uncertainty, $\sigma(z_{k-1}, z_k)$, using the average of the dense fixed-size bins that are within in the interval $[z_{k-1}, z_k]$. We also provide the mean residual error $\mathcal{L}^\rho = \frac{1}{|\mathcal{Z}|}\sum_{k\in\mathcal{Z}} \mathcal{E}(z_{k-1}, z_k)$ for facilitating the interpretation of the uncertainty error.

We compare UALE vs fixed-size approximation, when (a) f is piecewise-linear and (b) f is non-linear. In all examples, we execute $t = 30$ independent runs, using each time $N = 500$ different samples, and we report the mean values of the metrics.

Piecewise-Linear Function. Here, the black-box function is $f(\mathbf{x}) = a_1x_1 + x_1x_2$, with 5 different-width regions, i.e., a_1 equals to $\{2, -2, 5, -10, 0.5\}$ in the intervals defined by the sequence $\{0, 0.2, 0.4, 0.45, 0.5, 1\}$. We are interested in the effect and the uncertainty of x_1 which are $f_\mu^{\mathcal{GT}}(x_1) = a_1x_1$ in the regions defined above and $f_\sigma^{\mathcal{GT}}(x_1) = \sigma_2x_1$, respectively.

As we observe in the top left of Figure 5, UALE's bin-splitting separates the fine-grained bins, e.g., intervals $[0.4, 0.45]$, $[0.45, 0.5]$, and unites (most of) constant-effect regions into a single bin, e.g. region $[0.5, 1]$. This explains the fact that UALE achieves lower MAE $\mathcal{L}^\mu$, $\mathcal{L}^\sigma$ compared to fixed-size bins for all K.

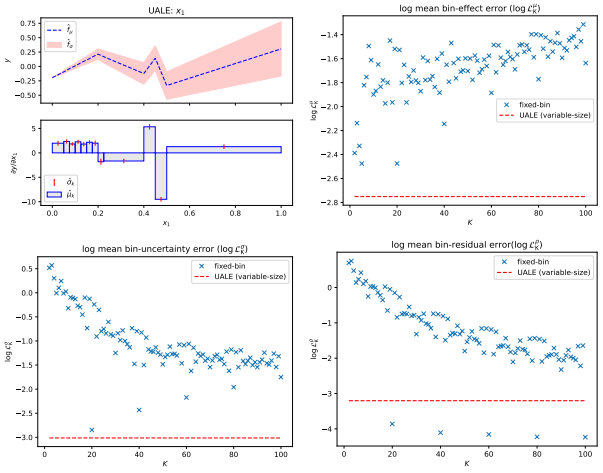

Figure 5: Bin-Splitting, piecewise-linear function: UALE's approximation (Top-Left). UALE vs fixed-size approximations in terms of: $\mathcal{L}^\mu$ (Top-Right), $\mathcal{L}^\sigma$ (Bottom-Left), $\mathcal{L}^\rho$ (Bottom-Right).

Non-Linear Function. Here, the black-box function is $f(\mathbf{x}) = 4x_1^2 + x_2^2 + x_1x_2$, so for x_1 the effect is $f_\mu^{\mathcal{GT}}(x_1) = 4x_1^2$ and the uncertainty is $f_\sigma^{\mathcal{GT}}(x_1) = \sigma_2x_1$. Due to the non-linear effect, wide bins (low K) increase the mean residual error, $\mathcal{L}^\rho$, making the uncertainty approximation biased. This can be clearly observed in in the bottom-right of Figure 6. On the other hand, narrow bins (high K) lead to worse approximation due to the limited number of samples. Interestingly, UALE's bin splitting manages to compromise these conflicting objectives and provides an accurate estimation, as we see in the bottom-left of Figure 6.

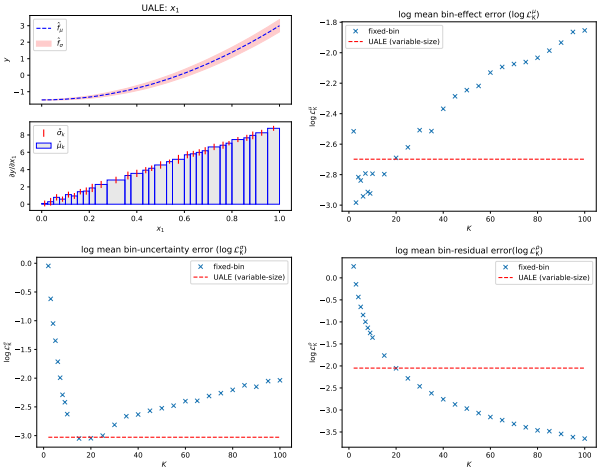

Figure 6: Bin-Splitting, non-linear function: UALE's approximation (Top-Left). UALE vs fixed-size approximations in terms of: $\mathcal{L}^\mu$ (Top-Right), $\mathcal{L}^\sigma$ (Bottom-Left), $\mathcal{L}^\rho$ (Bottom-Right).

5 REAL-WORLD EXAMPLE

Here, we aim at demonstrating the usefuleness of uncertainty quantification and the advantages of UALE's approximation, on the real-world California Housing dataset (Pace and Barry, 1997).

ML setup The California Housing is a largely-studied dataset with approximately 20000 training instances, making it appropriate for robust approximation with large K. The dataset contains $D = 8$ numerical features with characteristics about the building blocks of California, e.g. latitude, longitude, population of the block or median age of houses in the block. The target variable is the median value of the houses inside the block in dollars that ranges between $[15, 500] \cdot 10^3$, with a mean value of $\mu_Y \approx 201 \cdot 10^3$ and a standard deviation of $\sigma_Y \approx 110 \cdot 10^3$.

We exclude instances with missing or outlier values and we normalize all features to zero-mean and unit standard deviation. We split the dataset into $N_{tr} = 15639$ training and $N_{test} = 3910$ test examples (80/20 split) and we fit a Neural Network with 3 hidden layers of 256, 128 and 36 units respectively. After 15 epochs using the Adam optimizer with learning rate $\eta = 0.02$, the model achieves a MAE of $37 \cdot 10^3$ dollars.

Below, we illustrate the feature effect for three features: latitude x_2, population x_6 and median income x_8. The particular features cover the main FE cases, e.g. positive/negative

trend and linear/non-linear curve, and are therefore appropriate for illustration purposes. Results for all features, along with in-depth information about the preprocessing, training and evaluation parts are provided in the Appendix.

Uncertainty Quantification In real-world datasets, it is infeasible to obtain the ground truth FE for evaluation. We observe in Figure 7 that UALE and PDP-ICE compute, roughly, a similar average effect and uncertainty. Note that when the average effect remains (almost) constant in a wide interval, i.e., the feature effect plot is linear, UALE creates a single bin for this interval, which facilitates the interpretation. This can be observed, in the bottom plots of Figure 7, in the interval $x_8 \in [1.5, 6]$.

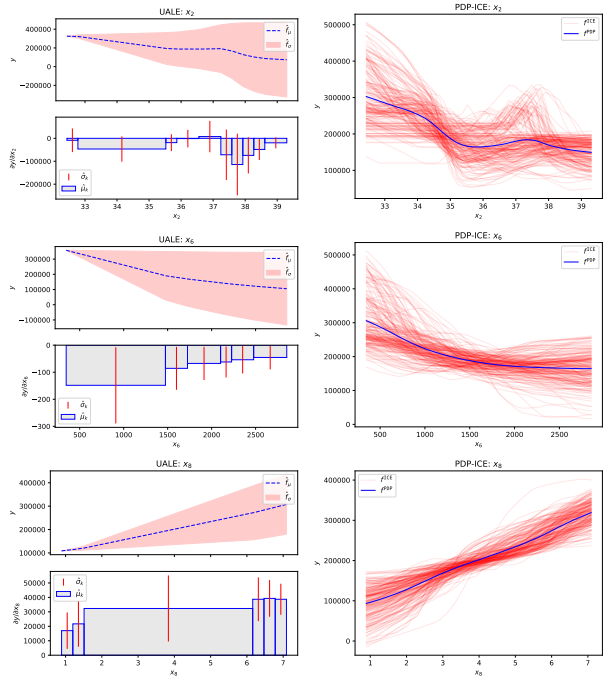

Figure 7: Real-dataset, UALE (left column) vs PDP-ICE (right column) for features x_2, x_6, x_8 (top to bottom).

Bin Splitting We evaluate the robustness of UALE approximation, following the evaluation framework of Section 4.2. We treat as ground-truth the effects computed on the full training set ($N_{tr} = 15639$) with dense fixed-size bin-splitting ($K = 80$). Given the sufficient number of samples, we make the hypothesis that the approximation with dense binning is close to the ground truth. Afterwards, we randomly select fewer samples, $N = 1000$, and we compare UALE approximation against fixed-size approximation (for all K). We repeat this process for $t = 30$ independent runs and we report the mean values of $\mathcal{L}^{\mu}, \mathcal{L}^{\sigma}$. In Figure 8, we observe that UALE achieves accurate approximations in all cases; the MAE of the uncertainty $\mathcal{L}^{\sigma}$ is close to the best of the fixed-size approximations.

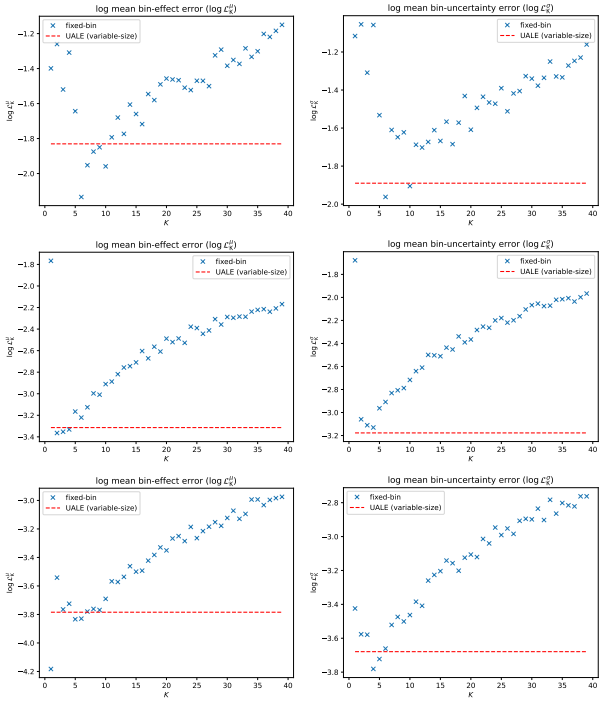

Figure 8: Real-dataset, UALE vs fixed-size approximation in terms of $\mathcal{L}^{\mu}$ (left column), $\mathcal{L}^{\sigma}$ (right column) for features x_2, x_6, x_8 (top to bottom).

6 CONCLUSION AND FURTHER WORK

We have introduced UALE, a method that extends ALE by quantifying the uncertainty of the global feature effect. To do that, UALE uses the standard deviation of instance-level effects. We showed that UALE models the uncertainty of feature effect more accurately than existing methods, such as ICE plots, especially in cases where there are dependencies between features. Providing an unbiased estimate of the uncertainty of the feature effect, however, is not trivial. In the case of ALE and the approximation of the average global effect, splitting the feature domain in K equal-width bins is sufficient. For estimating the uncertainty, however, we proved that this approach would introduce bias. We overcame this limitation by proposing an algorithm for automatically determining the optimal variable-size partitioning considering the instance-level effects. We show, through both synthetic and real-world examples, that UALE is an effective method for modeling both the average effect and the uncertainty.

There are certain limitations and open issues in the proposed approach. First, finding the optimal bin partitioning can be computationally expensive, if applied directly to ALE. By using DALE's approximation this limitation is resolved, however this is directly applicable only for differentiable models. Furthermore, UALE quantifies only the standard deviation of instance-level effects, providing lim-

ited intuition about the sources of the uncertainty. Future work should therefore aim at developing methods for identifying which features and to what degree contribute to the heterogeneity of instance-level effects.

Acknowledgments

All acknowledgments go at the end of the paper, including thanks to reviewers who gave useful comments, to colleagues who contributed to the ideas, and to funding agencies and corporate sponsors that provided financial support. To preserve the anonymity, please include acknowledgments *only* in the camera-ready papers.

References

Daniel W Apley and Jingyu Zhu. Visualizing the effects of predictor variables in black box supervised learning models. *Journal of the Royal Statistical Society: Series B (Statistical Methodology)*, 82(4):1059–1086, 2020.

Hubert Baniecki, Wojciech Kretowicz, and Przemyslaw Biecek. Fooling partial dependence via data poisoning. *arXiv preprint arXiv:2105.12837*, 2021.

Matthew Britton. Vine: visualizing statistical interactions in black box models. *arXiv preprint arXiv:1904.00561*, 2019.

Jerome H Friedman. Greedy function approximation: a gradient boosting machine. *Annals of statistics*, pages 1189–1232, 2001.

Jerome H Friedman and Bogdan E Popescu. Predictive learning via rule ensembles. *The annals of applied statistics*, pages 916–954, 2008.

Vasilis Gkolemis, Theodore Dalamagas, and Christos Diou. Dale: Differential accumulated local effects for efficient and accurate global explanations. *arXiv preprint arXiv:2210.04542*, 2022.

Alex Goldstein, Adam Kapelner, Justin Bleich, and Emil Pitkin. Peeking inside the black box: Visualizing statistical learning with plots of individual conditional expectation. *journal of Computational and Graphical Statistics*, 24(1):44–65, 2015.

Brandon M Greenwell, Bradley C Boehmke, and Andrew J McCarthy. A simple and effective model-based variable importance measure. *arXiv preprint arXiv:1805.04755*, 2018.

Ulrike Grömping. Model-agnostic effects plots for interpreting machine learning models, 03 2020.

Julia Herbinger, Bernd Bischl, and Giuseppe Casalicchio. Repid: Regional effect plots with implicit interaction detection. In *International Conference on Artificial Intelligence and Statistics*, pages 10209–10233. PMLR, 2022.

Scott M Lundberg, Gabriel G Erion, and Su-In Lee. Consistent individualized feature attribution for tree ensembles. *arXiv preprint arXiv:1802.03888*, 2018.

Ninareh Mehrabi, Fred Morstatter, Nripsuta Saxena, Kristina Lerman, and Aram Galstyan. A survey on bias and fairness in machine learning. *ACM Computing Surveys (CSUR)*, 54(6):1–35, 2021.

Christoph Molnar, Giuseppe Casalicchio, and Bernd Bischl. Interpretable machine learning–a brief history, state-of-the-art and challenges. In *Joint European Conference on Machine Learning and Knowledge Discovery in Databases*, pages 417–431. Springer, 2020a.

Christoph Molnar, Gunnar König, Bernd Bischl, and Giuseppe Casalicchio. Model-agnostic feature importance and effects with dependent features–a conditional subgroup approach. *arXiv preprint arXiv:2006.04628*, 2020b.

R Kelley Pace and Ronald Barry. Sparse spatial autoregressions. *Statistics & Probability Letters*, 33(3):291–297, 1997.